CROATICA CHEMICA ACTA CCACAA 63 (3) 373—399 (1990)

CCA-1946

YU ISSN 0011-1643
UDC 541-183
Conference Paper (Invited)

Contrasting Surface Behavior of Rh (111) and Pt (111) Electrodes*

*M. Hourani,** M. Wasberg, C. Rhee, and A. Wieckowski****

Department of Chemistry, University of Illinois,
1209 W. California St., Urbana, Illinois 61801

Received May 4, 1990

Low energy electron diffraction and voltammetric measurements of the Rh (111) electrode were conducted and compared with the corresponding surface and electrochemical characteristics of Pt (111). Rhodium is *unstable* upon exposure to water vapor or liquid water, but retains its well-defined character after immersion to aqueous media. This is reflected in the voltammetric behavior of the clean surface, as well as the manner in which carbon monoxide and iodine are adsorbed from solution. That is, a monolayer of an oxygen-containing species, assembled into (2×2) surface structure, can either be reduced by the voltammetric treatment or replaced by adsorbing solution components without causing system disorder. The voltammetry of the Rh (111) electrode, while exhibiting the main features of several metallic single crystal surfaces, differs significantly from that of platinum electrodes normalized to the same 2D geometry. From the voltammetric behavior, it is concluded that adsorption of high energy hydrogen is not taking place on Rh (111). Equally important, the packing density and the surface structure of the Rh (111) — CO differs from its Pt (111) — CO analog. While iodine chemisorption from the gas phase leads to the development of several surface structures known from the corresponding platinum work, preferential formation of the Pt (111) $(\sqrt{3} \times \sqrt{3})$ R30°—I structure against the Pt (111) $(\sqrt{7} \times \sqrt{7})$ R19.1°—I was demonstrated. Both electronic and structural factors contribute to the contrasting surface behavior brought to focus in this work.

INTRODUCTION

Among catalytic electrode materials, platinum has received the bulk of the attention. The need for providing molecular-level information focused on this electrode is extensive since the understanding of the rationale behind its distinctive properties will help to design advanced, economically attractive electrocatalysts for the future. Likewise, the structure of the electrical double

---

* Based on an invited lecture presented at the *8th »Ruđer Bošković« Institute's International Summer Conference on the Chemistry of Solid/Liquid Interfaces* Red Island, Rovinj, Croatia, Yugoslavia, June 22 — July 1, 1989.

** Present address: University of Jordan, Amman, Jordan.

*** To whom correspondence should be addresed.

layer on platinum is the object of active investigatons. Compared to the double layer on such metals as mercury, platinum distinguishes itself by showing a strong affinity for chemisorption and by providing numerous surface-assisted, reactive routes.

To better understand the surface electrochemistry of platinum, the pattern of behavior exhibited by this metal should be analyzed in the proper context of the properties of other electrode materials. The most challenging case appears to be rhodium. Until recently, the lack of proper research tools has prevented surface electrochemists from acquiring proper insight into the matter on the level easily accessible in gas phase surface science. A change in emphasis from polycrystalline rhodium to corresponding single-crystal systems,[1-6] and the development of several new methodologies, is revolutionizing the scope and depth of »liquid phase« surface science. In particular, the successful combination of UHV techniques with electrochemical circuitry,[7] *in situ* vibrational analysis of the liquid-solid adsorbates,[8] as well as radioactive labeling techniques[9] enable the researchers to compare the chosen electrochemical materials with the analog system created under gas phase conditions. The goal of this work is to present such a comparison for the case of Pt(111) and Rh(111) electrodes, studied predominantly by the combined UHV-electrochemistry technique. We will show that this single-crystal work reveals some similarities, but also profound differences in the molecular-level characteristics of the similar »noble« electrodes with identical crystallographic orientation.

EXPERIMENTAL

The ultra-high vacuum/electrochemistry transfer system which incorporates electron spectroscopies for surface analysis and electrochemical circuitry in a single apparatus has recently been reported[10] (Figure 1). The electrode is cleaned *in vacuo* and immersed in the electrolytic solution for adsorption and electrochemical characterization. The transfer from the electrolyte to UHV (and reverse) is conducted under argon overpressure, *i. e.*, without exposure to the atmospheric ambient. Using a meniscus-type configuration (Figure 2) the crystal surface is characterized through voltammetry and exposed to the electrolyte-containing individual adsorbing molecules dissolved in 0.1 M $HClO_4$ at a predetermined bulk concentration. Following a given time of adsorption, the cell is flushed with clean supporting electrolyte and/or water, the system is evacuated and the adsorbate-covered surface LEED analyzed at 10^{-8} Torr (the base pressure of our instrument is in the low 10^{-10} Torr regime).

The Rh (111) single crystal was obtained from the Materials Preparation Facility of Cornell University. The crystal was mechanically polished by diamond paste (Buehler) to 0.25 μm and the orientation of the crystal was confirmed to be within $\pm 1^0$ by X-ray back reflection. While in vacuum, the Rh (111) sample was cleaned by repeated Ar^+ bombardment (1 KeV, $\simeq$ 4 ηA ion current) at 5×10^{-5} Torr for 15 minutes followed by vacuum annealing at $\simeq$ 800 °C. The crystal was further annealed for 20 minutes in a 3×10^{-8} Torr oxygen atmosphere followed by 5 minutes of annealing without oxygen. This cycle was repeated until the order and cleanliness of the surface was confirmed by the use of LEED and Auger spectroscopy (see Results).

All measurements were conducted ar room temperature. Potentials are given *vs.* an Ag/AgCl reference with $[Cl^-] = 1$ M (the actual concentration of chloride was 10^{-5} M and the potentials are recalculated to the 1 M Cl^- concentration accordingly). Chemicals were A. R. grade, 18 MΩ Millipore water was used, and gases were supplied by Linde Specialty Gases. A PAR 273 potentiostat/galvanostat was used along with a BAS X—Y recorder for the voltammetric data acquisition.

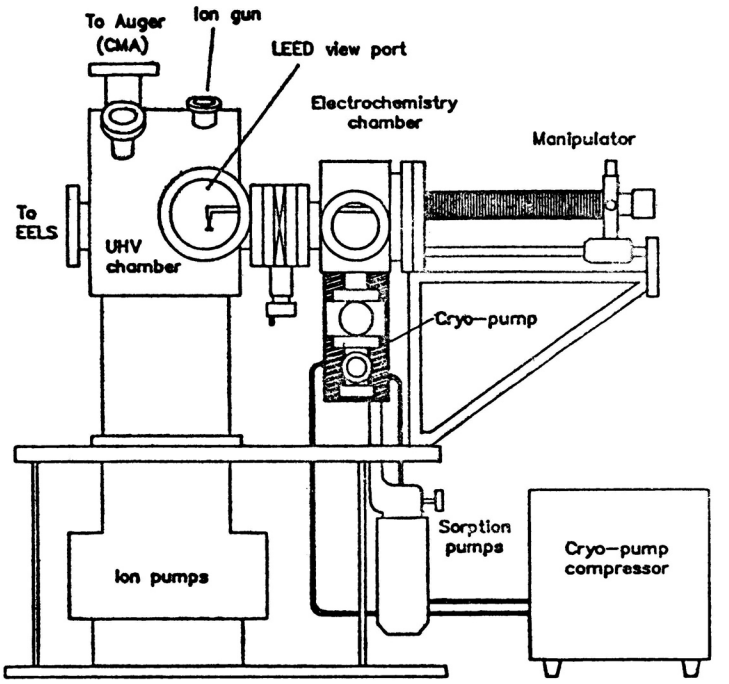

Figure 1. The sketch of the UHV-electrochemistry system and its components.

RESULTS

1. *Surface Science Characterization of Clean Rh(111) and Pt (111) Substrates*

Following ion bombardment and annealing in O_2-atmosphere and in O_2-free UHV environments, the Rh(111) and Pt(111) surfaces exhibited a proper hexagonal LEED pattern, and Auger analysis indicated only negligible surface contaminants, as shown in Figures 3 and 4, respectively. The surfaces were stable in the UHV environment for many hours, indicating that our instrument was contamination-free or that the electrode surfaces were inert toward vacuum impurities. Surfaces displaying the proper LEED/Auger characteristics were used for the adsorption/electrochemistry measurements reported below.

2. *Surface Cleanliness and Stability Test of the Rh (111) Electrode. Oxidation of Rhodium*

Since the essential feature of this work was the electrochemical characterization of the vacuum prepared single crystal surface of rhodium, a test was required to prove that the vacuum/gas and subsequent gas/liquid pahse transfer does not lead to contamination and experimental artifacts. That this is not the case for Pt(111) has been reported previously,[7,10-13] and corresponding

assays for Rh(111) have been conducted in this study along the following lines:

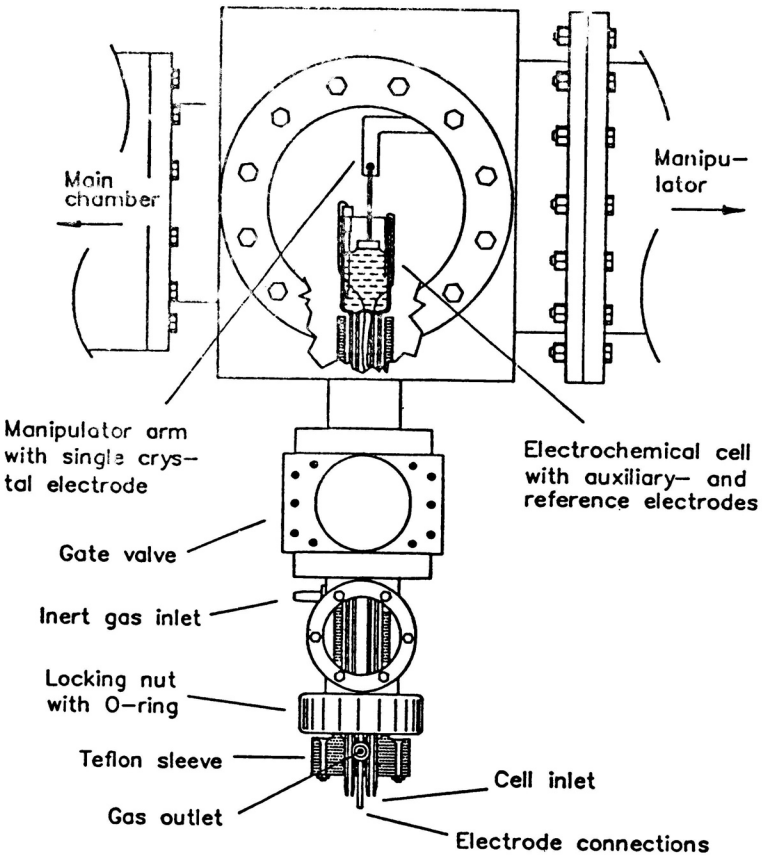

Figure 2. A schematic view of the electrochemistry chamber and electrochemical cell showing the meniscus arrangement for isolation of the monocrystalline surface of the electrode.

Test #1. The metal surface was exposed to clean argon in the electrochemistry chamber and transferred back to the to the main analytical chamber for LEED/Auger characterization. Fulfilling this scheme, no changes were observed by LEED and no noticeable deviation from the basic Auger spectrum (Figure 3) were observed. That is, the surface could be assumed intact.

Test #2. The clean Rh(111) surface was positioned for several seconds above a glass cell filled with Millipore water and returned to UHV for the electron spectroscopy analysis. When this procedure had been completed, a LEED pattern distinctly different from the (1 × 1) pattern was observed and is presented in Figure 5-A. That is, we conclusively document that an adlattice of a chemisorbed species was created. The only detectable difference in Auger signal following the H_2O water exposure was that located in the electron energy

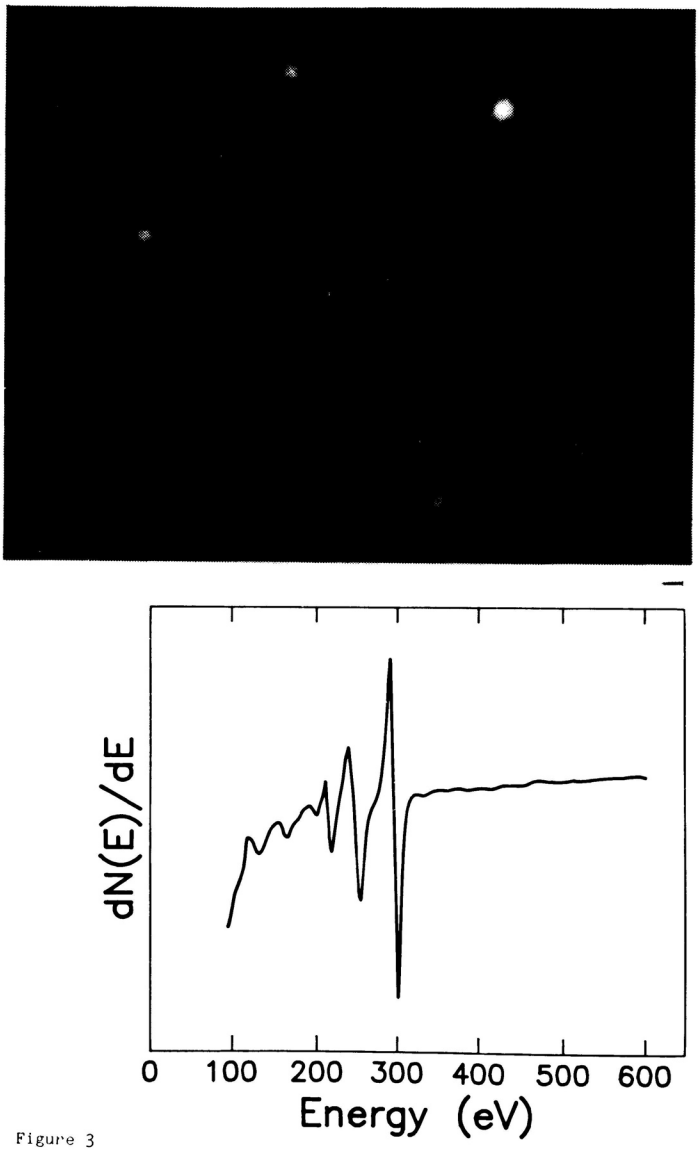

Figure 3

Figure 3. Low energy electron diffraction pattern of lean Rh(111) electrode, E = 65 eV. Auger electron spectrum of the same Rh(111) surface. Primary beam energy: 2.0 kV, crystal current: 8 μA. Modulation amplitude 6 V. Scan rate 1 mV/s.

range above 500 eV (Figure 6) and could unequivocally be assigned to surface oxygen. That is, *the rhodium surface was unstable upon exposure to an inert gas (argon) containing several Torr of water vapor.* This property of the rhodium surface deviates from the well known behavior of platinum which remains stable under the above conditions.[7,10-13]

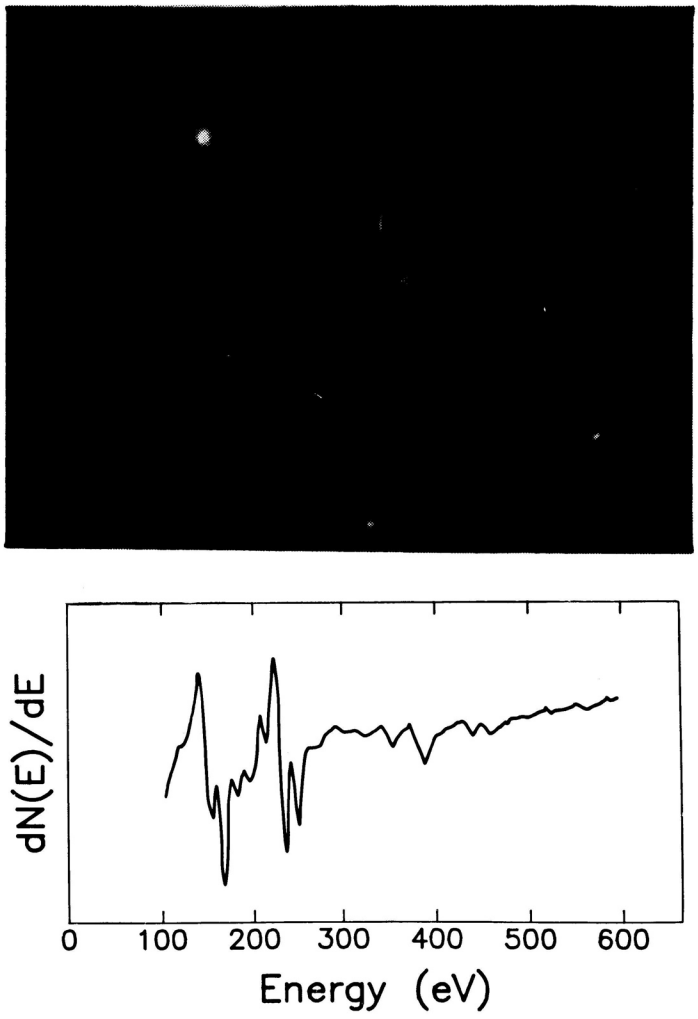

Figure 4. Low energy electron diffraction pattern of clean Pt(111) electrode, $E = 65$ eV. Normal incidence Auger electron spectrum of the same Pt(111) surface. Primary beam energy: 2.5 kV, crystal current: 21.2 μA. Modulation amplitude 4 V. Scan rate 1 mV/s.

Test #3. The Rh(111) electrode was immersed in clean water and, following evacuation, the surface was LEED/Auger analyzed. After this procedure, a very similar LEED pattern (Figure 5-B) to that shown in Figure 5-A was obtained and an only somewhat larger oxygen Auger signal was recorded as compared to that shown in Figure 6. This shows that the oxidation process due to vapor exposure is approaching saturation level. Immersing the crystal into a 0.1 M perchloric acid solution gave the same LEED pattern (Figure 5-B), however, the Auger spectrum indicated that a submonolayer of chlorine was present on the surface. Since the chlorine signal was absent if

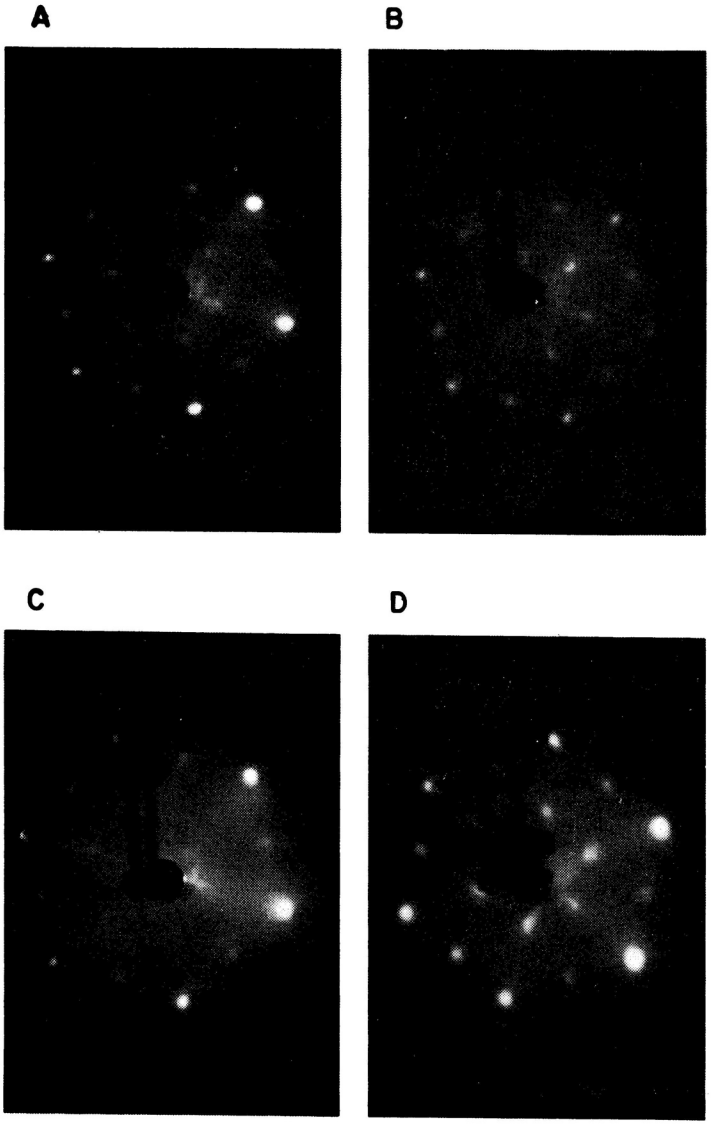

Figure 5. Low energy electron diffraction patterns of Rh(111) surface after: (A) exposure to water vapor, $E = 50.3$ eV; (B) dipping in water, $E = 60.7$ eV; (C) the electrode potential excursion in 0.1 M $HClO_4$ to a potential of 0.44 V, followed by emersion of the electrode at this potential, $E = 62.1$ eV; (D) adsorption of oxygen gas phase at 2×10^{-7} Torr for 30 s, $E = 62.9$ eV.

the perchlorate exposure was preceded by clean water exposure, the procedure of water immersion before electrolyte immersion was used throughout this study.

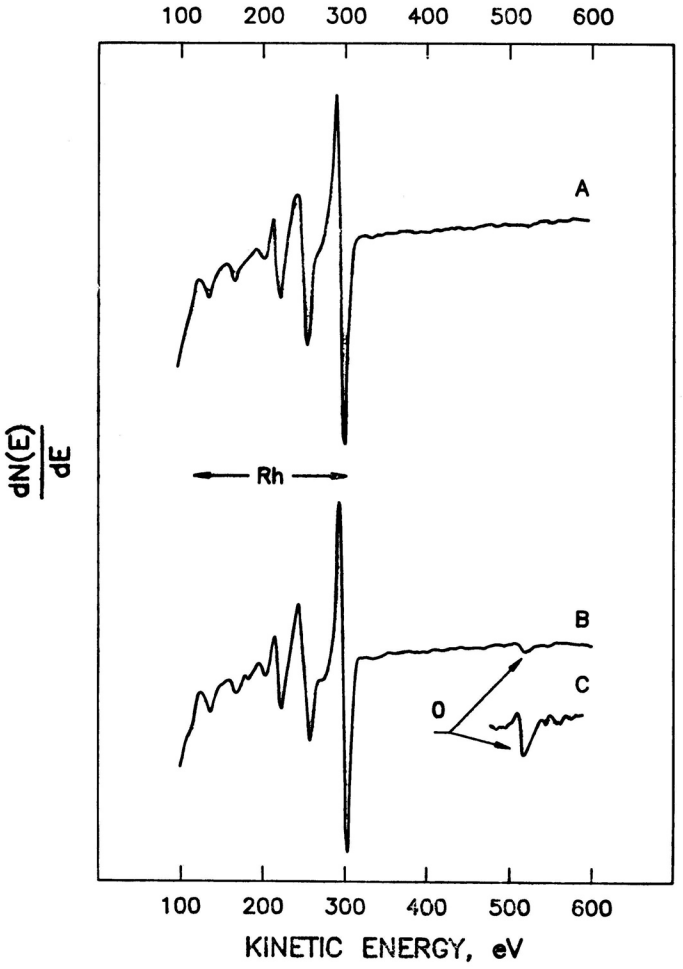

Figure 6. Auger electron spectra. (A) clean Rh(111); (B) Rh(111) (2 × 2)-ox (where ox is an oxygen containing species). Scan rate 1 eV/s; excitation amplitude (peak to peak): 6 V; primary beam current: 8 μA; primary beam energy: 2 keV.

Figure 5-C shows a LEED pattern of the Rh(111) surface obtained after the electrode *immersion* in 0.1 M $HClO_4$ (the rest potential of 0.2 V), and an electrode potential excursion to, and *emersion* at, 0.44 V. This latter potential value coincides with the end of the peak shown on the voltammogram of the Rh(111) electrode in the potential range of 0.3 to 0.5 V (see below and Figure 7). Again, the only discernible Auger signal except for those for rhodium was that assignable to surface oxygen. For the sake of comparison with the pat-

terns shown in Figures 5-A-C, the Rh(111) surface was dosed from gas phase with oxygen at $2 \cdot 10^{-7}$ Torr. Again, the (2×2) LEED pattern was observed (Figure 5-D). This pattern is known from analog gas phase studies by other authors.[14-18]

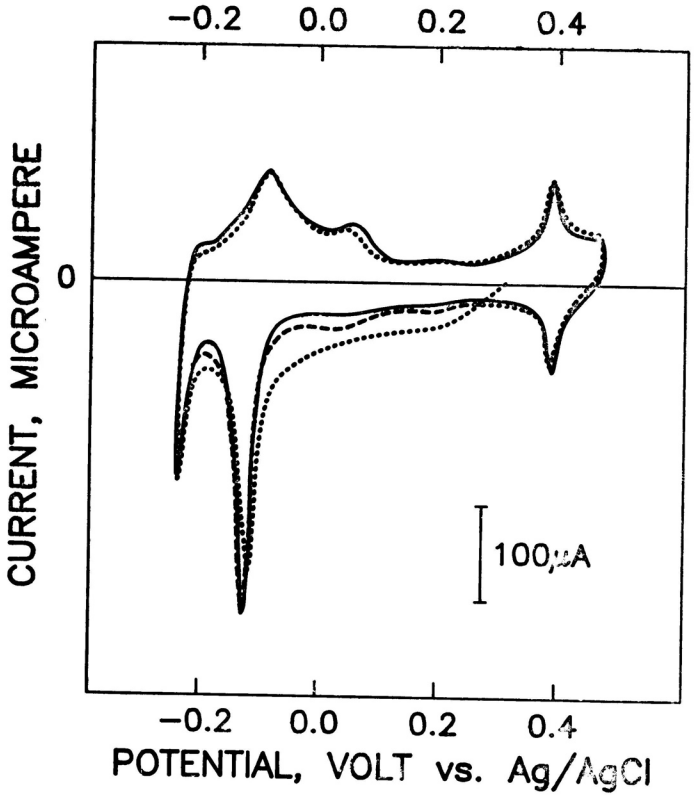

Figure 7. Cyclic voltammograms of Rh(111) electrode in 0.1 M $HClO_4$ showing the first scan starts negatively from the rest potential (the dotted line). The second cycle is represented by a dashed line, and the steady-state voltammogram is shown as the solid line. Geometrical surface area = 0.95 cm^2; scan rate 50 mV/s.

Figure 7 shows the voltammetric curve for the Rh(111) electrode recorded upon the first negative-going scan which was taken directly after the UHV prepared electrode was immersed in supporting electrolyte. The starting potential coincided with the rest potential of the system (0.2 V). The data show a typical case of irreversible electrochemical behavior with no counter peak observed affer the scan reversal at the onset of the hydrogen evolution. The area difference taken as that under the first and the second (stable) current-potential curves shows the occurrence of a reduction process in excess of the regular hydronium ion reduction in the potential range of —0,1 to —0.2 V. The calculated extra charge was equal to 280 $\mu C/cm^2$. This corresponds to an irreversible reduction of a monolayer of adsorbed species

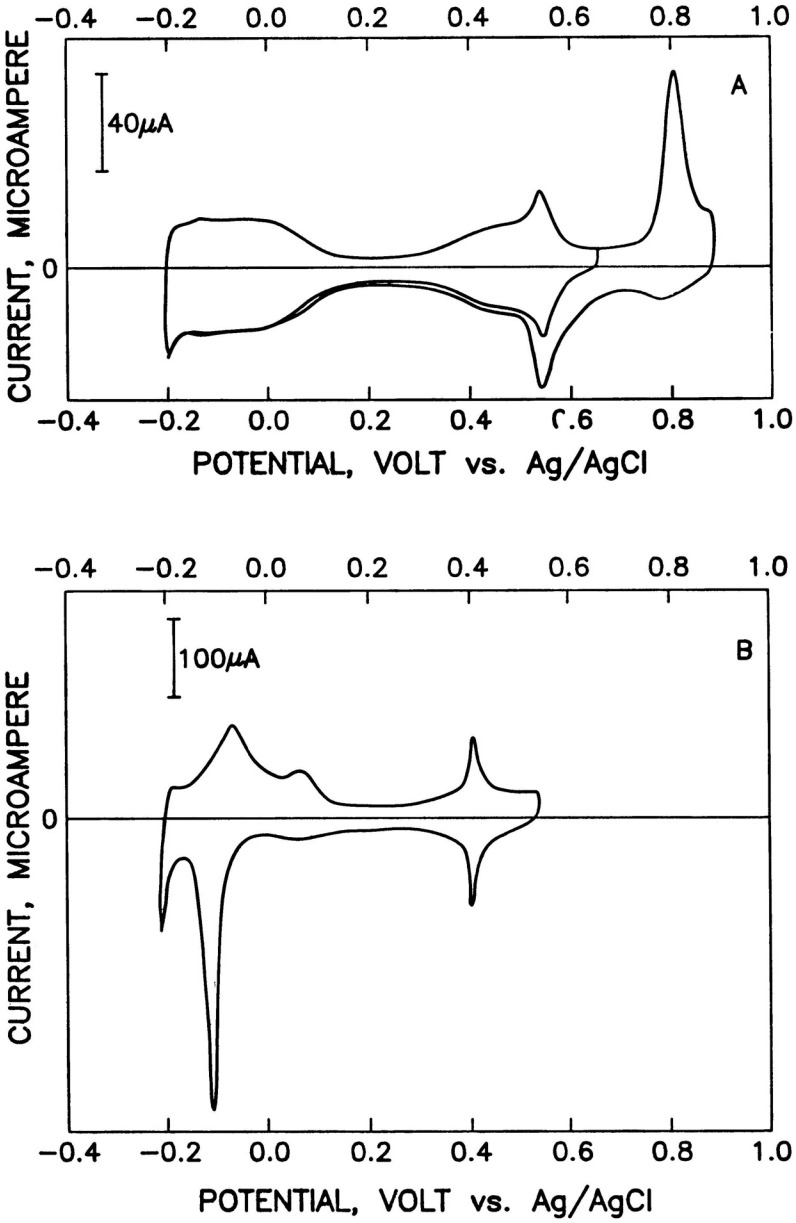

Figure 8. Cyclic voltammograms in 0.1 M $HClO_4$ recorded at 50 mV/s of UHV-prepared (A) Pt(111), (B) Rh(111).

in a reaction involving a one-electron transfer, or one-half monolayer in a two-electron reduction process.

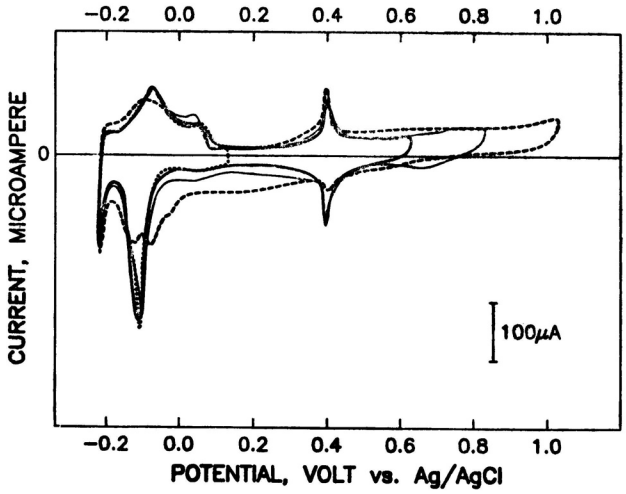

Figure 9. A window opening experiment with Rh(111) in 0.1 M $HClO_4$ at 50 mVís. The anodic switching potential increases in the positive direction.

Summing up this part of our work, we notice that following water or electrolyte exposure, an oxide film is formed on the rhodium surface. However, *the formation of this oxide film does not disorder the metal surface* as indicated by the absence of intensity loss of the integral LEED spots and the lack of a noticeable increase in the background scattering.

3. *Voltammetry of the UHV-Prepared Pt (111) and Rh (111) Surfaces (Order/Disorder Transitions)*

The voltammograms of the clean Pt(111) and Rh(111) electrodes are compared in Figure 8. We found that neither a loss of sharpness of the LEED spots, nor an increase in the background intensity of the LEED electrons appeared due to the potential cycling in the corresponding potential ranges. That is, no loss of long range surface order occurred on either of the two surfaces due to this voltammetric treatment. The characteristic feature in the Rh(111) voltammogram is the presence of a spike at 0.42 V. This spike is shifted by 120 mV in the negative direction against its platinum analog.[19] The hydrogen adsorption behavior is basically different between the two systems, with much more irreversibility exhibited by Rh(111) *vs.* Pt (111).

Window opening measurements with the UHV-prepared rhodium are shown in Figure 9. It is seen that increasing the positive value of the reversal potential above $E = 0.9$ V brings about a significant change in the morphology of the voltammogram. That is to say, the hydrogen part of the curve is losing its sharpness, and Clavilier's equivalent properties[19] in the more positive

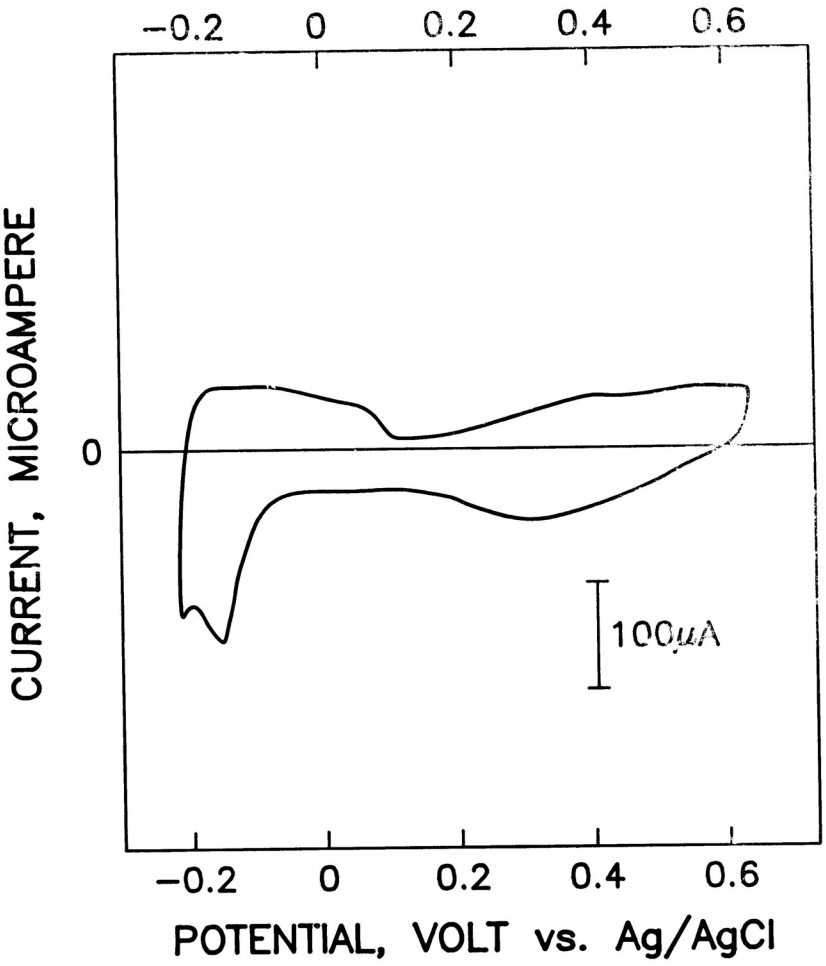

Figure 10. The voltammogram of the Rh(111) electrode after the potential was cycled from — 0.2 to 1.2 V in 0.1 M $HClO_4$. See Figure 9.

potential range (peak at 0.2 V) are becoming significantly modified. After several cycles in the potential range from —0.2 to 1.2 V, a final, repeatable voltammogram is shown in Figure 10. No LEED pattern was observed following system emersion of such a severely oxidized surface, which indicates total surface disorder, and a lack of periodicity characheristic for the well-defined Rh(111) electrode. This confirms our earlier conculsions regarding order/disorder properties of Rh(111) which were arrived at based upon earlier results obtained by electrochemistry,[1,2] *i.e.* without application of the ultra-high vacuum procedures used in this work. Similar behavior of Pt(111) has already been reported.[20]

4. *Adlattices: Carbon Monoxide and Iodine*

4.1. Electrosorbed CO

LEED patterns, surface structures and voltammetry of carbon monoxide electrosorbed on Pt(111) have recently been published by our laboratory[13] (Figures 11,12-A). Corresponding investigations focused on Rh(111) have been carried out in this study as described below.

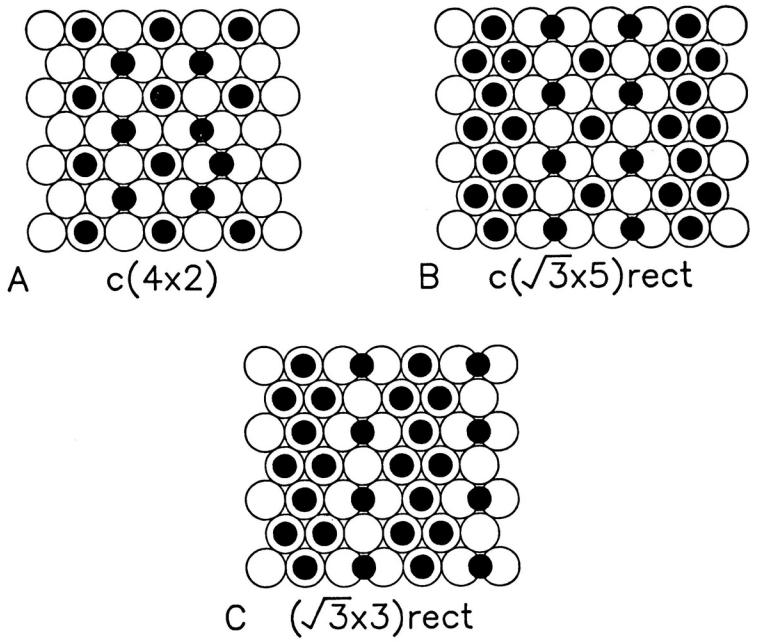

Figure 11. Structures of CO adsorbed on Pt(111) discussed in Ref. 13. (A) c (4 × 2), $\Theta = 0.5$; (B) c ($\sqrt{3} \times 5$) rect, $\Theta = 0.6$; (C) ($\sqrt{3} \times 3$) rect, $\Theta = 0.67$.

Carbon monoxide was adsorbed on a vacuum prepared Rh(111) surface, the cell was rinsed with supporting electrolyte, and a cyclic voltammogram was taken in the solution free of carbon monoxide. In Figure 12-B, such a voltammogram shows a single irreversible current-potential (c-p) peak centered at 0.46 V. The peak displays tailing-type behavior, which is in contrast to the surface CO oxidation on Pt(111)[13] which yields a symmetric response (Figure 12-A). The integration of the c-p curve under this peak (Figure 12-B) gave a charge of 383 $\mu C/cm^{-2}$, which leads to a packing density of 0.75, as already reported by Weaver *et al.*[21] Interestingly, six voltammetric scans within the potential limits shown in Figure 12-B were needed to restore the initial (and representative) voltammogram of the Rh(111) surface, which may indicate a significant disorder due to CO oxidation. The healing mechanism due to the voltammetric treatment is at present unknown. We note, however, that an analog disorder-type of behavior was not observed with the Pt(111)/CO system under analogous experimental conditions.[13]

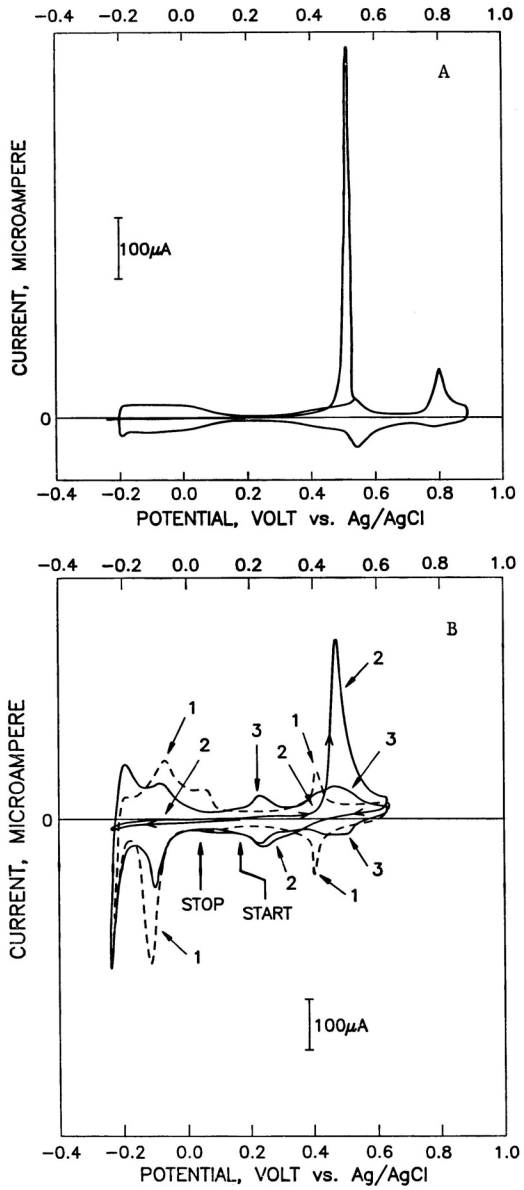

Figure 12. Electrooxidation of a saturation coverage of CO in CO-free 0.1 M $HClO_4$ electrolyte; (A) on Pt (111) electrode and (B) Rh (111) electrode. Carbon monoxide was adsorbed at 0.15 V from the electrolyte saturated with 0.1 M $HClO_4$. Scan rate 50 mV/s. 1) the voltammogram of a clean Rh (111) surface; 2) the stripping scan of chemisorbed CO; 3) the scan taken after potential reversal of scan 2.

The effect of evacuation down to the 10^{-8} Torr level on the stability of the CO adlattice was checked by emersing the Rh(111) surface saturated with

CO to vacuum at the 10^{-8} Torr level. After returning to the electrolytic environment, the linear sweep voltammogram was taken, starting from the rest potential, and is demonstrated in Figure 13. The electrochemical determination of the CO packing density again shows a value close to 0.75, the same as without UHV exposure. That is, no desorption of carbon monoxide was detected. However, the voltammetric peak assignable to the CO electrooxidation is somewhat broader than the one without the emersion procedure depicted above. Nevertheless, the tailing character of the c-p morphology is well preserved and the similarities between the plots shown in Figures 12-B and 13 outnumber the differences. An even closer morphological, current-potential resemblance was observed with the *in situ* and UHV exposed Pt(111)-CO systems, and has recently been reported.[13]

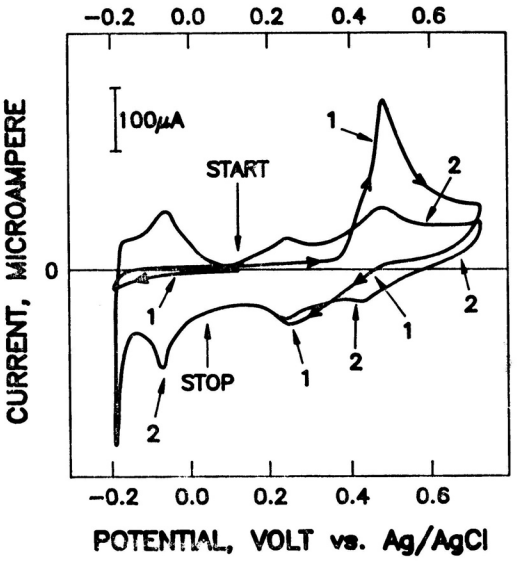

Figure 13. Electrooxidation of a saturation coverage of CO adsorbed on Rh(111) after exposure to the ultra-high vacuum environment for 5 minutes. For comparison see Figure 12-B.

In another experiment, carbon monoxide was potentiostatically adsorbed from the CO-saturated electrolyte at 0.1 V to obtain a saturation packing. After emersion, Auger analysis indicated equal occupancy on the surface of oxygen and carbon. This shows conclusively that the rhodium oxide initially present on the surface due to water exposure was quantitatively removed before the CO adlattice was established. Reduction or displacement of the Rh-O by solution carbon monoxide evidently occurred. While some beam damage of the CO adlattice was observed,[13] this adverse effect was easily controlled by minimizing the time of the electron irradiation, observing the LEED patterns at the very first moment of the screen illumination, and empolying low current Auger analysis in the Auger energy range of the expected elements.

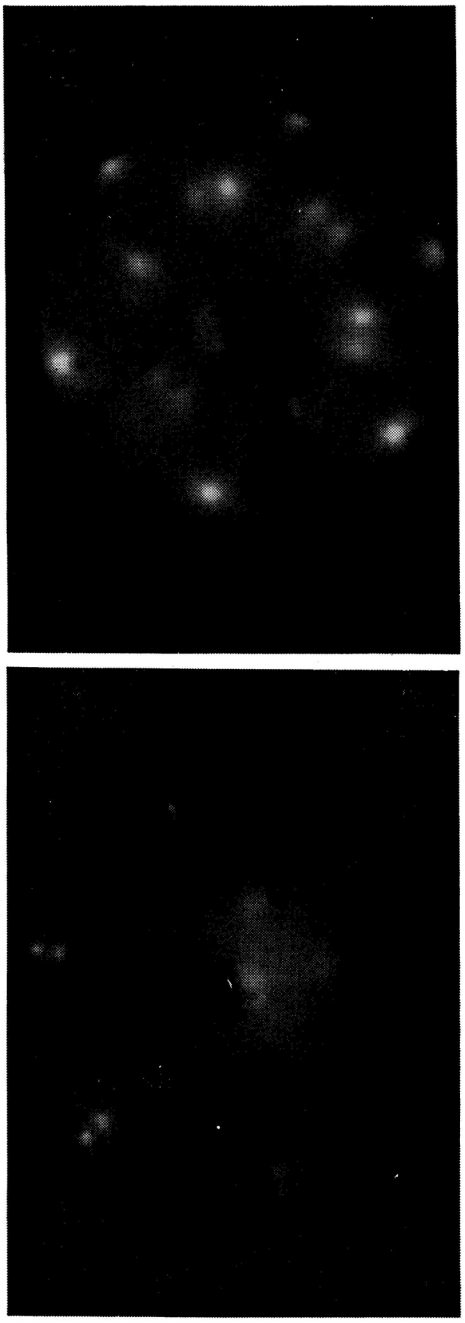

Figure 14. Low energy electron diffraction patterns of CO adsorbed on Rh (111). CO was adsorbed at 0.15 V from CO-saturated 0.1 M $HClO_4$ (A) $E = 49.2$ eV, (B) $E = 38.0$ eV.

The LEED of the Rh(111)-CO surface at the saturation coverage obtained under our conditions (0.75) shows a split (2×2) pattern (Figure 14). This pattern was previously reported by Somorjai *et al.*[14,22,23] after CO adsorption from the gas phase ($0.33 < \Theta < 0.75$). The Rh(111) (2×2) pattern at $\Theta = 0.75$, also observed by the cited authors, has not been found in this study.

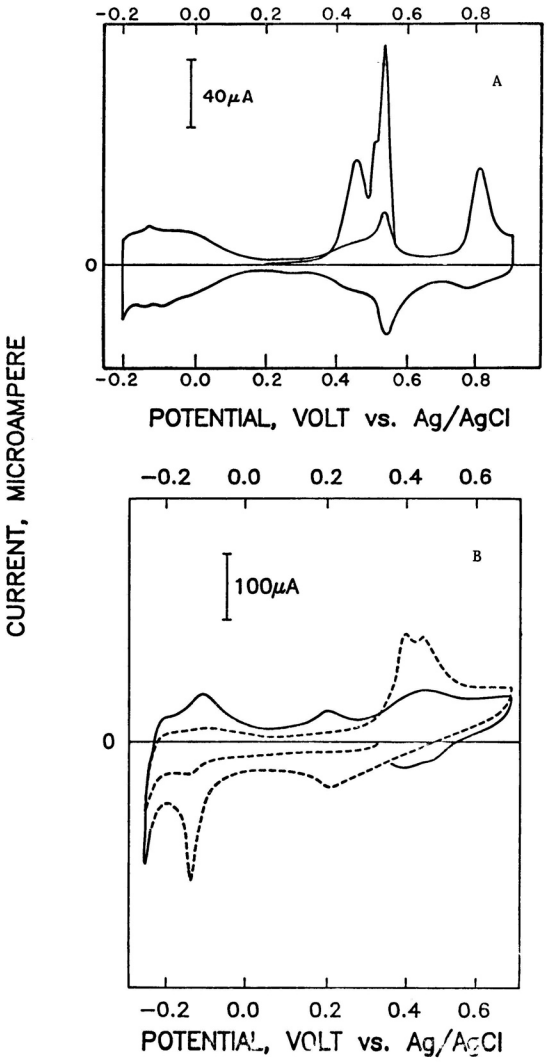

Figure 15. (A) Electrooxidation of submonolayer coverage of CO adsorbed on Pt(111) as in Ref 13. (B) Electrooxidation of submonolayer coverage of CO adsorbed on Rh(111) ($\Theta = 0.45$). Supporting electrolyte: 0.1 M $HClO_4$. Scan rate 50 mV/s.

Figure 15 shows the voltammograms of Pt(111) (Figure 15-A) and Rh(111) (Figure 15-B) electrodes which contain submonolayer packing of carbon monoxide. Dosing the Rh(111) surface with CO at a packing density of 0.45

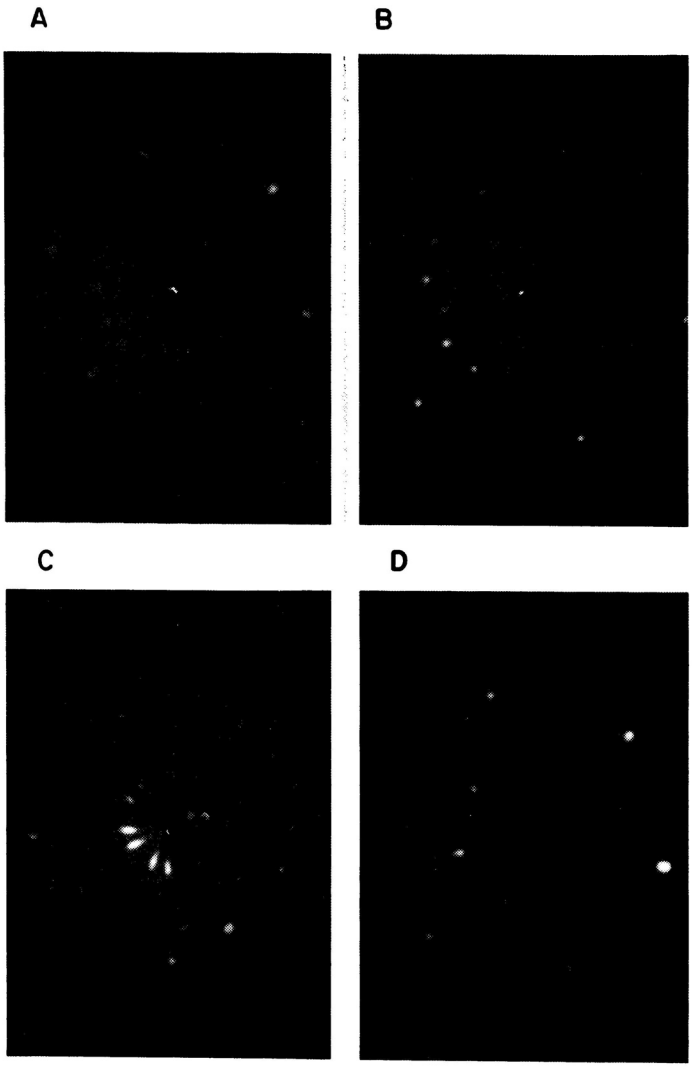

Figure 16. Low energy electron diffraction patterns of iodine adlattices formed on Rh(111) under UHV conditions. (A) Multiple domains structure (Rh(111) $(\sqrt{7} \times \sqrt{7})$ R19.1°—I + Rh(111) (3×3)—I, $E = 53.7$ eV; (B) multiple domains structure (Rh(111) $(\sqrt{7} \times \sqrt{7})$ R19.1°—I + Rh(111) $(\sqrt{3} \times \sqrt{3})$—I), $E = 51.6$ eV; (C) Rh(111) $(\sqrt{7} \times \sqrt{7})$ R19.1°—I, $E = 27.7$ eV and (D) Rh(111) $(\sqrt{3} \times \sqrt{3})$ R30°—I, $E = 46.2$ eV.

produces a characteristic peak splitting which vaguely corresponds to observations made with the Pt(111)/CO system[13] (Figure 15-A). The corresponding interpretation is given in the Discussion. No attempt was made to emerse partially covered Rr(111)-CO surfaces to vacuum, since the anticipated coad-

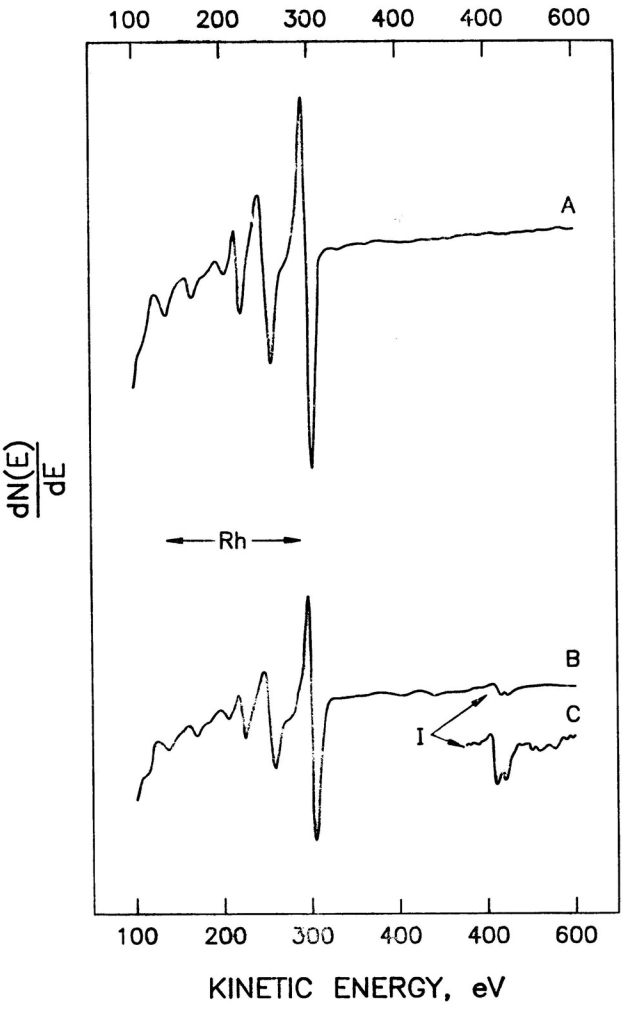

Figure 17. Auger electron spectra of (A) clean Rh(111); (B) Rh(111) ($\sqrt{7} \times \sqrt{7}$) R19.1°—I. Scan rate 1 eV/s; excitation amplitude (peak to peak): 6 V; primary beam current: 8 μA; primary beam energy: 2 keV.

sorption with surface oxygen would render the interpretation of the resulted surface composition difficult.

4.2. Adsorption of Iodine (Gas and Liquid Phase Dosing)

As in the case of the Pt(111) surface chemistry, several LEED patterns and convoluted surface structures of chemisorbed iodine were observed with progressively decreasing packing densities of the adsorbate (Figure 16). However, contrary to the equivalent measurements with Pt(111) done by Hub-

bard *et al.*, [24,25] the most easily obtained structure was that denoted as Pt(111) $(\sqrt{3} \times \sqrt{3})$ R30° — I, rather than Pt(111) $(\sqrt{7} \times \sqrt{7})$ R19.1° — I. That is a 10 L exposure was needed at 10^{-7} Torr level to see a clearly developed »$\sqrt{7}$« pattern (Figure 16-C). Auger analysis (Figure 17) focused on the

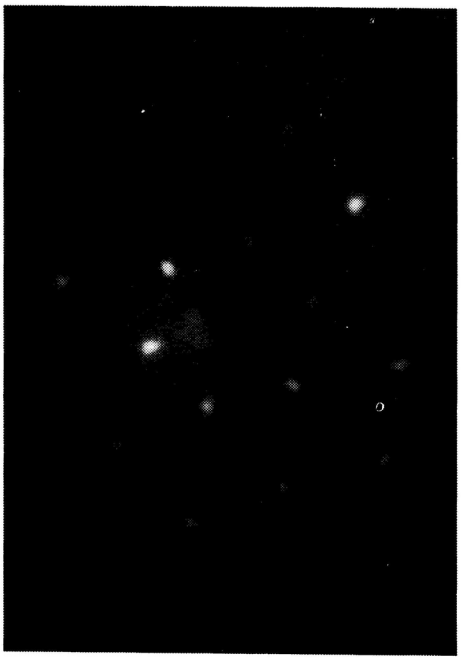

Figure 18. Low energy electron diffraction pattern, Rh(111) $(\sqrt{3} \times \sqrt{3})$ R30°—I, formed in solution after the clean and ordered Rh (111) surface was immersed in 1 mM KI. $E = 56.1$ V.

I-covered rhodium surfaces gave several iodine packing densities: 0.49, 0.43, and 0.34, which correspond to the following convoluted surface structures: a mixed pattern of $(\sqrt{7} \times \sqrt{7}) + (3 \times 3)$, $(\sqrt{7} \times \sqrt{7})$ R19.1° and $(\sqrt{3} \times \sqrt{3})$ R30° (Figures 16-A, 16-C and 16-D, respectively). A multidomain structure of $(\sqrt{7} \times \sqrt{7}) + (\sqrt{3} \times \sqrt{3})$ was also observed at $\Theta = 0.37$ (Figure 16-B).Except for the high coverage pattern of $\sqrt{7} + (3 \times 3)$, all the structures were also observed on Pt(111) upon vacuum dosing by iodine.[11,12,24] While the more densely packed surface structure was not observed on platinum upon dosing at $10^{-7}/10^{-8}$ Torr, it was found after dosing at atmospheric pressure in the instrumental configuration reported in ref. 26. That is, almost the same structural behavior of the two metals displaying the (111) orientation toward gas phase iodine was found in this study. Likewise, the structural reversibility[26] was confirmed by annealing the $\sqrt{7} + (3 \times 3)$ structure at 400° °C and

observing the structural transformations through $\sqrt{7}$, $\sqrt{7}+\sqrt{3}$, and $\sqrt{3}$. Complete desorption took place at approximately 900 K.

Chemisorption of iodine from a 1 mM solution of potassium iodate gave a $(\sqrt{3}\times\sqrt{3})$—I surface structure (LEED pattern, Figure 18). This is an interesting result since liquid exposure of Pt(111) to KI-solution at the same bulk concentration gave either the $\sqrt{7}$ or weak (3×3) surface structure.[25] That is, the $\sqrt{3}$ structure appears to be more stable on Rh(111) than on Pt(111) at the expense of the more highly packed adlattices. Oxygen was not present on the Rh(111) surface, as indicated by Auger, and no remnants of the (2×2) structure from adsorbed oxygen domains were seen. As in the case of the carbon monoxide, the final destiny of iodine is not affected by surface oxygen which is initially present on the surface due to the metal instability upon water exposure.

DISCUSSION

Contrary to platinum, but with some analogy to such active metals and alloys as iron[27] and stainless steel,[28] rhodium becomes oxidized upon exposure to water vapor or to liquid water. However, the oxidation does not disorder the surface as it does in the case of the more reactive materials. The oxygenous film appears thin on the molecular scale, and is composed of a monolayer of chemisorbed OH or O species. The fact that no surface disorder was encountered upon water exposure shows that single crystal surfaces of rhodium may be qualified as *well-defined* electrodes.

The crucial question now is how the presence of the surface oxygen directs the chemisorption behavior (and the initial surface reactivity) of rhodium in electrolytic media. From previous studies of rhodium surfaces it appears that the oxide film, while easily created, is susceptible to reduction.[14] In the case of an absence of reducing agents, as in the clean supporting electrolyte in use, the oxide monolayer can be reduced electrochemically by the application of a negative-going potential scan starting from the rest potential (dotted line, Figure 7). The extra charge measured between the first and the stable profile corresponds to a monolayer reduction of an adsorbate. Moreover, as inferred from the voltammetric features shown in Figure 7 and in Figure 8-B, the clean oxide-free surface is obtained after this electrochemical treatment. In addition to this conclusion, the results point to a very interesting difference in surface behavior of the dry and wet rhodium: the dry surface is oxidized by water exposure at room temperature (vapor or liquid) while the wet surface in the electrochemical configuration can be protected from the oxidation by choosing an appropriate potential regime. In other words, the dry surface behaves as if the metal were polarized to positive potentials, at least above the 0.4 V value, below which the electrochemical protection mechanism is activated. However, the properties of the dry and wet rhodium oxides are fundamentally different; the wet oxide is reversibly reduced at 0.42 V, while the dry oxide reduction needs potential excursion down to a value of —0.1 V. Therefore, a significant difference in the morphology and/or stoichiometry of the oxides formed from the gas phase or from aqueous solutions must exist, and we may postulate that the surface and oxide

film hydration plays an important role in this contrasting (dry *vs.* wet) behavior.

The present paper reports on the voltammetric properties of the ordered Rh(111) electrode in perchloric acid supporting electrolyte (Figures 7 and 8-B). As in the case of platinum electrodes, the Rh(111) voltammetric profiles differ from those of the polycrystalline electrode[1,2] and from disordered Rh(111).[29] On the quantitative end of the voltammetric analysis, it should be emphasized that the charge needed for hydrogen adsorption/desorption, 300 $\mu C/cm^2$, after converting to the number of surface sites active in adsorption, accounts for a full monolayer of adsorbed hydrogen.[29] An equivalent number for Pt(111), as reported by Clavilier[19] and others,[30,31] is 0.66; *i.e.* hydrogen chemisorption on the Rh(111) electrode is completed in a classic potential range of —0.2 to 0.1 V, while the surface of (111) platinum remains only fractionally hydrogen-covered at potentials preceding hydrogen evolution. To confront this situation, one is either forced to postulate a high energy hydrogen to occupy the remaining surface sites,[19] or argue that the water adlayer assumes unusual properties due to the ordering influence of the (111) crystallographic orientation.[30] Leaving the question of the Pt(111) voltammetry open to further research, it appears that there is no need to assume any other than regular form of electrosorbed hydrogen on Rh(111). This leads us to the conclusion that the spike at 0.42 V (Figure 7) is due to the initial stage of surface oxidation, which takes the form of a phase transition. No new LEED pattern is associated with this oxidation, compared to the (2 × 2) pattern developed due to simple water exposure. There is, therefore, a need for either a dynamic LEED, or an *in situ* surface analysis to provide a crystallographic description of the surface transformation in the potential range around 0.4 V.

The CO adsorption from aqueous electrolytes displays a close similarity to CO adsorbed from the gas phase.[14,22,23] It may therefore be concluded that the solid/liquid interface is a similar host for the CO molecules as is the metal/vacuum interface exposed to CO under vacuum dosing conditions. The exception is the lack of (2 × 2) surface structure observed upon gas-phase dosing which leads to a limiting packing density of 0.75.[22,23] Contrary to this observation, a saturation ($\sqrt{3} \times 3$) rect surface structure of electrosorbed CO was observed on Pt(111) upon adsorption from both environments (Figure 11-C). Remembering that electrochemical adsorption is a substitutional process with participation of »preadsorbed« water molecules, water interaction on the two metal surfaces in the vacuum and electrochemical (or equivalent) environments should now be more closely examined. While the desorption to vacuum from both metals takes place at a very similar temperature, the interaction between coadsorbed water and carbon monoxide on platinum differs from that on rhodium. Namely, as shown by Wagner *et al.*,[32,33] this interaction is hydrophilic on Rh(111) and hydrophobic on Ph(111). Therefore, it is energetitically easier to replace adsorbed water molecules by solution molecules on the latter surface than on the former. Such a discriminating energy barrier on Rh(111) may be especially difficult to transpass at the end of the replacement-chemisorption process, *i.e.*, when fully CO-coordinated H_2O molecules are exposed to solution CO. In view of our data and the above discussion, we conclude that the energy deficiency to transform the split Rh(111) (2 × 2) pattern to (2 × 2) results from the attractive forces between the coadsorbed

products on the Rh(111) electrode. The repulsion between water and carbon monoxide on Pt(111) facilitates the surface replacement, and the same saturation packing densities are obtained from both gas phase and solution environments.

In the context of the above discussion, we note that the electrooxidation of carbon monoxide on Rh(111) is facilitated as compared to that on (Pt(111) (*cf.* Figure 12-A and 12-B). The difference in the peak potentials of the CO oxidation equal to 50 mV gives an energy advantage of 10 kJ mol^{-1} in favor of rhodium. Since the coadsorbed water molecules are the source of oxygen needed for carbon monoxide electrooxidation to carbon dioxide, the hydrophilic interaction should, and does, facilitate the surface reaction. However, this comparison is made more complicated due to the overlap of both the CO and rhodium oxidation processes (Figure 12-B). The corresponding resolution of the two oxidation processes on platinum is much more favorable (Figure 12-A).

The split (2 × 2) LEED pattern was explained by Biberian and Van Hove[23] using the concept of antiphase domains. The surface structure can be visualized as a mixture of patches of $(\sqrt{3} \times \sqrt{3})$ R30° and (2 × 2) domains. According to this model, there is a regular transition between the $(\sqrt{3} \times \sqrt{3})$ R30° (or $(\sqrt{3} \times \sqrt{3})$ rect) to the (2 × 2) or c $(\sqrt{3} \times$ infinity), and the split structure can be labeled as c $(\sqrt{3} \times$ n), where n is an odd number: $3 < n < \infty$. The structure proposed by the authors cited above is shown in Figure 19.

The voltammogram or the Rh(111) surface containing 0.45 CO molecules per surface metal atom (Figure 15-B) shows two peaks centered at 0.41 and 0.46 V. Corresponding (and analogous) behavior of the Pt(111)-CO electrode has recently been reported (Figure 15-A).[13] By using the same arguments as in the paper cited above, the existence of at least two bonding configurations is now postulated. The *in situ* vibrational spectroscopy,[21] as well as the gas phase investigations,[23] led to the assignment of the weakly bound (electrooxidation at 0.41 V) to the bridge-type CO, and the strongly bound species to the terminal CO. While the significance of the fault-line molecules in the surface arrangement of the CO adlattice was strongly emphasized in the Pt(111) -CO system,[13] a corresponding analysis of the rhodium surface can not be made, void of the LEED data regarding the submonolayer CO structures. The *in situ* crystallographic data are needed to fill this gap in the intercomparison between the two surfaces.

The electrochemistry of iodine chemisorbed on Rh(111) and Pt(111) can be perceived as the case of near-perfect structural identity: most of the main surface structures already observed on Pt(111) have been found on Rh(111) (see Results). An exception is the $\sqrt{7}$ structure which was not observed after the Rh(111) exposure to the supporting electrolyte containing potassium iodide on the mM level. This structure was formed either on Pt(111) after the solution immersion, or after gas phase dosing on both Pt(111) and Rh(111) surfaces (Ref. 24 and Results). That is, this structure is stable in vacuum on both surfaces, and we may conclude that the $\sqrt{7}$ surface structure is not formed on the Rh(111) in the aqueous environments under the reported dosing condi-

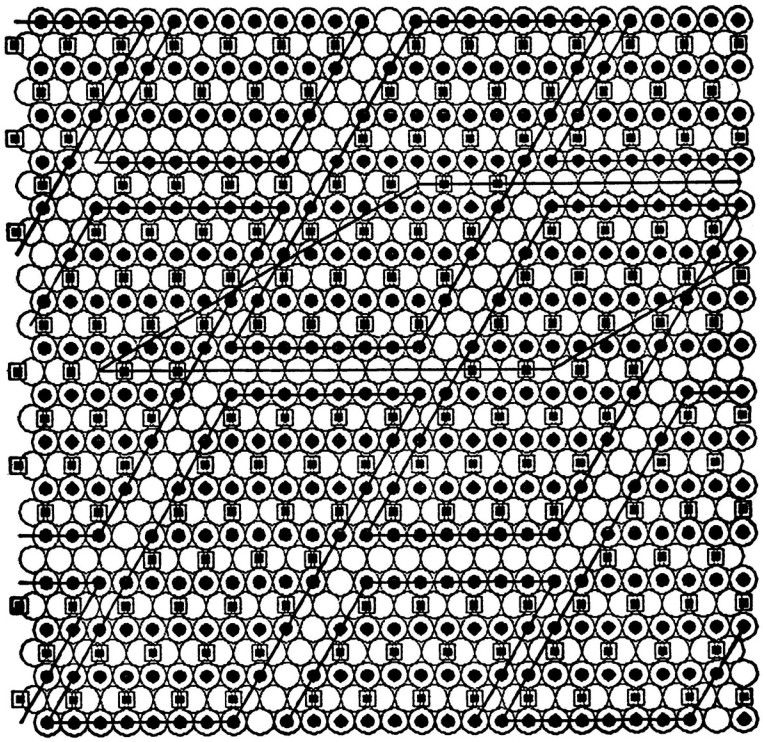

Figure 19. The Rh (111) -CO surface structure which yields the split (2 ×2) LEED pattern (Figure 14) as proposed by Biberian and Van Hove.[23]

tions. To account for this difference, one needs to remember that the distance of the closest approach for rhodium is *ca.* 3% shorter than for platinum (2.690 Å *vs.* 2.775 Å).[34] The resulting $\sqrt{7}$, I—I distance on the Rh(111) surface is equal to 4.109 Å, which gives the surface iodine a radius of 2.05 Å. This value is smaller than the van der Waals radius for iodine, which is equal to 2.15 A.[35] Packang densities greater than predicted from van der Waals's distances are generally not observed when adsorption is carried out under vacuum dosing conditions[24] (»atmospheric« dosing conditions are needed to observe higher surface coverages than those determined by the van der Waals restraints[26]). Evidently, in the filling of the Rh(111) surface in solution, the chemisorbing iodine is tarnspassing not only the chemical activation barrier (water replacement), but also the structural one (van der Waals compression). The two combined effects are concluded to account for the lack of Rh(111) $(\sqrt{7} \times \sqrt{7})$ — I structure formation in solution. Since the radius of the $\sqrt{7}$ iodine chemisorbed on Pt(111) and the van der Waals radius match almost perfectly, the van der Waals structural-type barrier on this metal is apparently negligible. As an effect, formation of the Pt(111) $(\sqrt{7} \times \sqrt{7})$ — I structure, either under the vacuum dosing conditions or from solution, occurs unhindered.

OVERVIEW AND CONCLUSIONS

The vacuum prepared, clean and ordered Rh(111) surface is chemically unstable upon exposure to either water vapor or liquid water. Nevertheless, the water treated, and thus oxidized surface can be characterized by electrochemistry and electron spectroscopy in conformity with the standards developed for studying single-crystal, well-defined electrodes. Therefore, our work broadens the arsenal of system which can reliably be approached by the ultra-high vacuum methodology and related techniques.

We compared the surface behavior of rhodium and platinum single-crystal electrodes normalized to the same crystallographic (111) orientation, and we report on the voltammetric behavior of such surfaces. From the voltammetric analysis, we conclude that the high energy hydrogen is not formed on rhodium (111). Likewise, we studied adsorption of iodine from both gas and solution phase on both metals. We demonstrated the significance of the 3% difference in the surface interatomic spacings between the two (111) metallic planes in the structural aspects of iodine adsorption from both gas and solution phase. Namely it appears that the formation of $(\sqrt{3} \times \sqrt{3})\,R30^0$ — I surface structure is more facilitated on rhodium (111) than on Pt(111). *En gross*, however, a near perfect structural identity of iodine chemisorbed on Rh(111) and Pt(111) was evidenced *via* our research.

We believe that the structural factors are responsible for the basically different LEED patterns (and corresponding surface structures) observed for the Rh(111)-CO and Pt(111)-CO. In particular, a specific »mosaic« of the CO antiphase domains and antiphase boundaries on Rh(111) may result from the 3% compression of the rhodium atomic network *vs.* the corresponding Pt(111) network. The role of the electronic factors in causing some fundamental differences in the surface behavior between platinum and rhodium have already been demonstrated *via* the analysis of hydrophilicity and hydrophobicity of the CO—H_2O interacting surface pairs. Consequently, we conclude that the lack of correspondence between the saturation surface structures of Rh(111)-CO produced from gas phase and solution phase, respectively, directly reflects the differences in the chemical nature of the CO—H_2O interactions. Indirectly, it reflects the differences in the electronic density distribution in the surface regions of the metals. A quantitative insight into the latter observations requires quantum mechanical analysis of the studied objects.

Acknowledgements. This works was supported by the National Science Foundation (DMR-86-12860) and by the Air Force Office of Scientific Research (AFOSR-89-0368).

REFERENCES

1. M. Hourani and A. Wieckowski, *J. Electroanal. Chem.* **227** (1987) 259.
2. M. Hourani and A. Wieckowski, *ibid.* **244** (1988) 147.
3. L. H. Leung, S. Chang, and M. J. Weaver, *J. Chem. Phys.* **90** (1989) 7426.
4. L. H. Leung and M. J. Weaver, *J. Phys. Chem.* **93** (1989) 7218.
5. F. T. Wagner, T. E. Moylan, and S. J. Schmieg, *Surf. Sci.* **195** (1988) 403.
6. M. Wasberg, M. Hourani, and A. Wieckowski, *J. Electroanal. Chem.*, in press.
7. A. T. Hubbard, *Acc. Chem. Res.* **13** (1980) 177.
8. A. Bewick and S. Pons in *Advances in Infrared and Raman Spectroscopy*, R. J. Clark and R. E. Hester (Eds.), New York, vol. 12, 1985, p. 1.

9. A. Wieckowski in *Modern Aspects of Electrochemistry*, J. O'M. Bockris, B. E. Conway, and R. E. White (Eds.), Plenum, New York, 1989, in press.
10. M. Wasberg, L. Palaikis, S. Wallen, M. Kamrath, and A. Wieckowski, *J. Electroanal. Chim.* **256** (1988) 51.
11. J. L. Stickney, S. D. Rosasco, D. Song, M. P. Soriaga, and A. T. Hubbard, *Surf. Sci.* **130** (1983) 326.
12. A. T. Hubbard, J. L. Stickney, S. D. Rosasco, M. P. Soriaga, and D. Song, *J. Electroanal. Chem.* **150** (1983) 165.
13. D. Zurawski, M. Wasberg, and A. Wieckowski, *J. Phys. Chem.* in press.
14. D. G. Castner, B. A. Sexton, and G. A. Somorjai, *Surf. Sci.* **71** (1978) 519.
15. P. A. Thiel, J. T. Yates, Jr., and W. H. Weinberg, *Surf. Sci.* **82** (1979) 22.
16. P. C. Wong, K. C. Hut, M. Y. Zou, and K. A. Mitchell, *Surf. Sci.* **165** (1986) L21.
17. T. W. Root and L. D. Schmidt, *Surf. Sci.* **134** (1983) 30.
18. M. A. Van Hove, R. J. Koestner, J. C. Frost, and G. A. Somorjai, *Surf. Sci.* **129** (1983) 482.
19. J. Clavilier, *J. Electroanal. Chem.* **107** (1980) 211.
20. A. T. Hubbard, *Chem. Rev.* **88** (1988) 633.
21. L.-W. Leung, S.-C. Chang, and M. J. Weaver, *J. Chem. Phys.* **90** (1989) 7426; L.-W. Leung and M. J. Weaver, *J. Phys. Chem.* **93** (1989) 7218.
22. L. H. Dubois and G. A. Somorjai, *Surf. Sci.* **91** (1980) 514.
23. J. P. Biberian and M. V. Van Hove, *Surf. Sci.* **138** (1984) 361.
24. T. E. Felter and A. T. Hubbard, *J. Electroanal. Chem.* **100** (1979) 473.
25. J. L. Stickney, S. D. Rosasco, G. N. Salaita, and A. T. Hubbard, *Langmuir* **1** (1985) 66.
26. A. Wieckowski, B. C. Schardt, S. D. Rosasco, J. L. Stickney, and A. T. Hubbard, *Surf. Sci.* **146** (1984) 115.
27. M. Kamrath, D. Zurawski, and A. Wieckowski, *Langmuir*, submitted.
28. D. A. Harrington, A. Wieckowski, S. D. Rosasco, G. N. Salaita, and A. T. Hubbard, *Langmuir* **1** (1985) 232.
29. M. Wasberg, M. Hourani, and A. Wieckowski, *J. Electroanal. Chem.*, in press.
30. F. T. Wagner and P. N. Ross, *J. Electroanal. Chem.* **250** (198) 31 (review).
31. P. Zelenay and A. Wieckowski in *In Situ Studies of Electrochemical Interfaces: A Prospectus*, H. D. Abruña (Ed.), in press (review).
32. F. T. Wagner, T. E. Moylan, and S. J. Schmieg, *Surf. Sci.* **195** (1988) 403.
33. F. T. Wagner and T. E. Moylan in *Electrochemical Surface Science: Molecular Phenomena at Electrode Surfaces*, M. P. Soriaga (Ed), ACS Symposium Series 378; American Chemical Society, Washington, DC, 1988, Chapter 5.
34. N. N. Greenwood and A. Earnshaw in *Chemistry of the Elements*, Pergamon, Oxford, 1984.
35. *CRC Handbook of Chemistry and Physics*, R. C. Weast and D. R. Lide (Eds.), CRC Press, Boca Raton, FL, 70th edition, 1989—1990.

SAŽETAK

Usporedba površinskog ponašanja Rh(111) i Pt(111) elektroda

M. Hourani, M. Wasberg, C. Rhee i A. Wieckowski

U cilju boljeg razumijevanja površinske elektrokemije platine, metala kojemu je u istraživanjima dosada posvećeno najviše pažnje, i uz nastojanja da se dobiju podaci na molekularnoj razini, istražuju se svojstva drugih srodnih elektrodnih materijala. Posebno rodij obećaje mnogo. Sve do nedavno je nedostatak odgovarajućih tehnika istraživanja sprečavao elektrokemičare u postizavanju onakvih informacija, koje su vrlo lako pristupačne istraživanjima u površinskoj fizici granice faza plin — metal. U ovom su radu obavljena mjerenja pomoću difrakcije niskoenergetskih elek-

trona (LEED) i voltametrijska mjerenja na Rh (111) elektrodama. Rezultati su uspoređeni s površinskim i elektrokemijskim podacima poznatim za Pt (111).

Voltametrijski podaci pokazuju da na Rh(111) ne dolazi do adsorpcije molekula vodika visoke energije. Gustoća adsorpcije i struktura Rh-CO sloja znatno se razlikuje u one Pt, iako je struktura Rh svega 3% gušća od atomske rešetke Pt. U adsorpciji jodid iona izmjerene su na Rh veće gustoće, nego što to predskazuju interakcije na osnovi van der Waals-ovih udaljenosti. To navodi na tumačenje da na Rh(111) jodid prelazi ne samo kemijsku aktivacijsku barijeru (zamjena molekula vode) nego i strukturalnu (van der Waals kompresija). Svi rezultati ukazuju da jednako elektronski kao i strukturalni činioci doprinašaju razlici u ponašanju površina tih dvaju metala.